ChemComm

Check for updates

The influence of exogenous amines on the electrochemical CO_2 reduction activity of a cobalt–pyridyldiimine catalyst†

Piyush Kumar Verma [a] and Charles C. L. McCrory [*ab]

Studying the interactions between CO_2 sorbents and electrocatalysts for the electrochemical CO_2 reduction reaction (e-CO_2RR) can offer viable strategies to advance the development of the Reactive Capture of CO_2 (RCC). In this report we studied the effect of amines on the performance of the [Co(PDI-Py)] catalyst for the e-CO_2RR. The presence of amines shifts the onset potential for the e-CO_2RR more positive and increases the catalytic activity while maintaining the high Faradaic efficiency ($\geq$90%) for CO production.

CO_2 capture from dilute sources such as flue gas and its fixation for later use is an important strategy in decarbonizing industry to minimize the net release of CO_2 into atmosphere.[1] In this carbon capture and utilization (CCU) process, CO_2 is captured by sorbents in the form of sorbent–CO_2 complexes and is used at later stages by reversing the capturing process upon thermal application. In essence, CCU enables the reuse or recycling of waste CO_2 to its higher value forms such as CO, HCOOH and MeOH. However, a major limitation of this strategy is that thermal release and concentration of CO_2 from sorbent–CO_2 adducts is an energy intensive process that limits the overall viability of CCU for achieving net zero carbon emissions.[2]

In contrast, the reactive capture of CO_2 (RCC) bypasses the need for CO_2 release by reducing the CO_2 while it is still adsorbed to the sorbent in its captured form, *e.g.* as a sorbent–CO_2 adduct. Hence, RCC is considered as a more energy efficient strategy compared to CCU.[3,4] RCC can describe three distinct processes: (a) the direct reduction of CO_2 in its sorbent-bound form into various products; (b) the *in situ* desorption and subsequent reduction of proximal CO_2 at the catalyst, and (c) the direct reduction of CO_2 from dilute (<1 atm) streams.

Several catalytic systems have been explored within this broad RCC framework in all areas of catalysis: thermal,[5,6] photocatalytic,[7,8] and electrocatalytic RCC.[9,10] State-of-the-art homogeneous RCC processes are thermal processes where *in situ* generated transition-metal hydrides reduce captured-CO_2 by amines/alkanolamines under an H_2 atmosphere.[5]

Electrocatalytic RCC (e-RCC) is a promising alternative to thermal RCC because e-RCC allows for the reduction of captured CO_2 under ambient conditions without high pressure H_2. However, the implementation of e-RCC with molecular electrocatalysts remains relatively underexplored. A notable example of homogeneous e-RCC was reported using an iron–phosphine complex that is reported to reduce CO_2 to methanol in the presence of diethylamine as co-catalyst.[11] The diethylamine is reported to react with CO_2 to form diethylammonium carbamate which is then electrochemically reduced to methanol with 68% Faradaic efficiency by the molecular catalyst. In another report, a Re–bipyridine complex is reported to reduce 1% CO_2 gas to CO with 85% Faradaic efficiency in the presence of triethanolamine. The triethanolamine is reported to react with CO_2 to form aminoethylcarbonate which coordinates to the Re-center and is subsequently reduced to generate CO.[12] Other insightful studies on the interactive effects of amines, phenol, and ionic liquids on catalyst systems for the electrochemical CO_2 reduction reaction (e-CO_2RR) underline the mechanisms through which the sorbents can affect the course of reaction either by acting as a ligand or by affecting the kinetics of the protonation steps involved in the catalysis.[13–16]
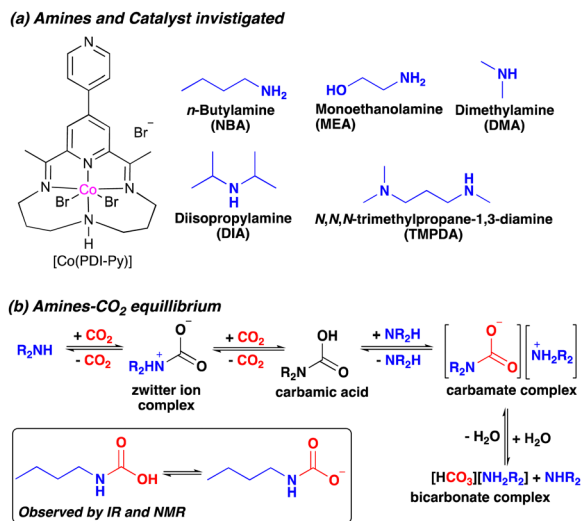
In this work, we report a new system for e-RCC based on a cobalt pyridyldiimine complex [Co(PDI-Py)] (Scheme 1a). We have shown previously that [Co(PDI-Py)] is active and selective for the e-CO_2RR to CO in CO_2-saturated acetonitrile (MeCN) solutions containing H_2O as a proton source.[17] Herein, we show that the e-CO_2RR activity of [Co(PDI-Py)] is enhanced when various aliphatic amines are added into the electrolyte solution (Scheme 1a). Specifically, adding primary or secondary aliphatic amines to a CO_2-saturated MeCN electrolyte solutions containing [Co(PDI-Py)] results in a favorable positive shift in

[a] Department of Chemistry, University of Michigan, Ann Arbor, Michigan, 48109-1055, USA. E-mail: cmccrory@umich.edu
[b] Macromolecular Science and Engineering Program, University of Michigan, Ann Arbor, Michigan, 48109-1055, USA

(a) Amines and Catalyst invistigated

n-Butylamine (NBA)

Monoethanolamine (MEA)

Dimethylamine (DMA)

[Co(PDI-Py)]

Diisopropylamine (DIA)

N,N,N-trimethylpropane-1,3-diamine (TMPDA)

(b) Amines-CO₂ equillibrium

R_2NH $\overset{+\ CO_2}{\underset{-\ CO_2}{\rightleftharpoons}}$ zwitter ion complex $\overset{+\ CO_2}{\underset{-\ CO_2}{\rightleftharpoons}}$ carbamic acid $\overset{+\ NR_2H}{\underset{-\ NR_2H}{\rightleftharpoons}}$ carbamate complex

$-\ H_2O$ $\Vert$ $+\ H_2O$

$[HCO_3][NH_2R_2]$ + NHR_2 bicarbonate complex

Observed by IR and NMR

Scheme 1   (a) Amines studied in this work and (b) amine-CO₂ equilibrium.

Fig. 1   Representative CVs of 0.3 mM Co(PDI-Py) in MeCN with 0.1 M nBu₄NPF₆ at a scan rate of 0.05 V s⁻¹. CVs were taken in Ar-sparged solution (gray line), CO₂-saturated solution containing 11 M H₂O (red line), and CO₂-saturated solution containing 11 M H₂O and 0.2 M NBA (blue line). The inset is a zoom in of the region in the dashed orange box showing the $Co^{3+/2+}$ and $Co^{2+/+}$ peaks.

the e-CO₂RR catalytic onset potential and an increase in the magnitude of the electrocatalytic current while maintaining high Faradaic efficiencies for CO production of $FE(CO) \geq 90\%$. The amines react with CO₂ in solution to form different CO₂ adducts that exist in equilibrium, including alkylammonium carbamate salts (Scheme 1b). However, attempts to directly reduce carbamate salts in the absence of added CO₂ result in a lower Faradaic efficiency of $FE(CO) \approx 16\%$, possibly because the equilibration of carbamate salt results in the lower effective concentration of carbamate and substantial concentration of free amine which can suppress the overall catalytic activity. Our results offer crucial insights for the development of effective e-RCC catalytic systems based on amines, which are prominently used industrial sorbent.

Cyclic voltammograms (CVs) of [Co(PDI-Py)] in Ar-sparged MeCN electrolyte show four reversible redox features assigned to two metal-based reductions ($Co^{3+/2+}$ and $Co^{2+/+}$) followed by two ligand-based reductions (PDI-Py/PDI-Py•⁻ and PDI•⁻/PDI-Py²⁻) (Fig. S4 and Table S1, ESI†). When the electrolyte is sparged with CO₂ and 11 M H₂O is added, the reductive current increases, indicative of a catalytic process with a catalytic onset near the PDI-Py/PDI-Py•⁻ couple (Fig. 1). Presence of H₂O enhances the catalytic rate for CO₂RR and stability of the catalyst as we observed in our previous studies of [Co(PDI-Py)].[17] After the amine NBA is added to the CO₂-saturated electrolyte solution containing [Co(PDI-Py)] and 11 M H₂O, we observe an increase in the magnitude of the catalytic current ($i_{c,amine}/i_c = 1.78$) and a ~0.18 V positive shift in the catalytic onset potential (Fig. 1). Similar responses were also observed for the e-CO₂RR by Co(PDI-Py) in presence of other amines (Fig. S5–S10, ESI†). The catalytic onset potential (E_{onset}) and ratio of the catalytic CO₂RR peak current with amine present and without amine present ($i_{c,amine}/i_c$) are summarized in Table 1. The presence of amines resulted in a positive shift in E_{onset} by ~0.18–0.14 V, and varying degrees of electrocatalytic enhancement from a high of $i_{c,amine}/i_c = 1.78$ for NBA to the lowest enhancement of $i_{c,amine}/i_c = 1.23$ for MEA.

Table 1   Effect of Amines on the Redox Potentials and CO₂RR activity of [Co(PDI-Py)] in CO₂-sparged solutions with 11 M H₂O[a]

Added amine	$E_{1/2}(Co^{3+/2+})/$ V *vs.* Fc⁺/⁰	$E_{1/2}(Co^{2+/1+})/$ V *vs.* Fc⁺/⁰	$E_{onset}/$ V *vs.* Fc⁺/⁰	$I_{c,amine}/$ i_c
No amine	−0.07	−0.85	−1.61	—
NBA	−0.46	−0.85	−1.43	1.78
MEA	−0.39	−0.85	−1.46	1.23
DMA	−0.43	−0.87	−1.47	1.69
DIA	−0.41	−0.85	−1.47	1.62
TPDA	−0.36	−0.86	−1.46	1.34
Aniline	−0.09	−0.85	−1.61	1.0

[a] CV experiments were performed with 0.3 mM [Co(PDI-Py)] in CO₂-saturated solution of 0.1 M nBu₄NPF₆ and 11 M H₂O in MeCN with a scan rate of 0.05 V s⁻¹. For experiments with amines, the concentration of the amine was 0.2 M.

Note that the addition of NBA to the CO₂-saturated solution with [Co(PDI-Py)] and 11 M H₂O also results in a −0.39 V shift in the $Co^{3+/2+}$ couple, but no observable shift in the $Co^{2+/+}$ couple as seen in the Fig. 1, inset for NBA, and for all amines in Fig. S5–S10 (ESI†). The resulting $E_{1/2}$ for the $Co^{3+/2+}$ couples and the unchanged $Co^{2+/+}$ couple in the CO₂-saturated solutions with 11 M H₂O are summarized in Table 1. These results suggest coordination of the carbamate species to the charged Co(III)-complex, but that the extent of coordination may not be as significant in the Co(II)-complex. Note that noncatalytic CVs of [Co(PDI-Py)] conducted in Ar-sparged CH₃CN electrolytes showed no significant change in peak heights or peak potentials upon the addition of amines (Fig. S11–S15 and Table S2, ESI†), suggesting that the coordination to the Co-complex observed in the CO₂-saturated solution is from the carbamate formed from the reaction of CO₂ and amine, and not from the free amine.

Fig. 2 Representative CVs of 0.3 mM Co(PDI-Py) in MeCN with 0.1 M nBu$_4$NPF$_6$ and 11 M H$_2$O at scan rate of 0.05 V s^{-1} with varying concentrations of NBA. The inset is the zoomed in region in the dashed orange box showing the e-CO$_2$RR catalytic response.

The tolerance of an electrocatalyst to higher concentration of sorbent is an important prerequisite for the practicality of an e-RCC system. It is expected that increasing the concentration of sorbent in solution should proportionally increase the partitioning of CO$_2$ into the solution, therefore increasing the activity of the catalytic system. We investigated the e-CO$_2$RR activity for [Co(PDI-Py)] in CO$_2$-saturated MeCN electrolyte solutions as a function of NBA concentration (Fig. 2). Most noticeably, there is a proportional increase in the magnitude of the catalytic peak for competitive HER at ~ -2.4 V $vs.$ Fc$^{+/0}$. When we zoom into the catalytic peak for the CO$_2$RR at ~ -1.6 V $vs.$ Fc$^{+/0}$, we observe a decrease in activity with increasing NBA concentration (Fig. 2, inset). We observe a similar trend of decreasing CO$_2$RR activity with increasing amine concentration for the other amines investigated (Fig. S16–S19, ESI†). We attribute this decrease in CO$_2$RR activity to the possible coordination of free amines in solution to [Co(PDI-Py)].

To confirm that the catalytic peak at ~ -1.6 V $vs.$ Fc$^{+/0}$ is due to the e-CO$_2$RR to CO, we conducted controlled potential electrolysis (CPE) experiments at -1.69 V $vs.$ Fc$^{+/0}$ in previously described gastight, two-chamber H-cells (ESI,† Experimental methods).[17] Representative current $vs.$ time plots of the CPE experiments in the presence of 0.05 M of each amine studied are shown in Fig. S20–S25 (ESI†), and the results from the CPE experiments are summarized in Table 2. The Faradaic efficiency for CO production is FE$_{CO} \geq 95\%$ regardless of the nature of the amine present. The highest activity is observed in the presence of NBA based on the charge passed during the CPE (Table 2) and the $i_{c, \text{amine}}/i_c$ ratio (Table 1). However, there is no clear trend between the size of the added amine and the measured CO$_2$RR activity. For comparison, CPEs conducted of [Co(PDI-Py)] in CO$_2$-saturated solutions with 11 M H$_2$O but no amine present also showed only CO production with FE$_{CO} \geq 90\%$, but with much less charge passed during the electrolyses. Post-CPE analysis of the working electrode by SEM-EDS

Table 2 Summary of CPE results for the CO$_2$RR by [Co(PDI-Py)] in CO$_2$-saturated solutions with 11 M H$_2$O^a

Amine	Charge/C	FE(CO)/%	FE(H$_2$)/%	Cobalt weight %
No amine	-2.6 ± 0.2	90 ± 11	Trace	0.13 ± 0.06
NBA	-8.2 ± 0.4	99 ± 12	2.9 ± 0.9	0.17 ± 0.06
MEA	-5.8 ± 0.6	98 ± 3	1.7 ± 0.5	0.07 ± 0.06
DMA	-5.2 ± 0.7	98 ± 7	1.6 ± 0.4	0.20 ± 0.20
DIA	-5.5 ± 0.4	97 ± 2	1.4 ± 0.2	0.33 ± 0.06
TMPDA	-4.9 ± 0.8	95 ± 6	2.8 ± 1.6	0.03 ± 0.05

^{a} All CPE experiments were conducted at -1.69 V $vs.$ Fc$^{+/0}$ for 30 min in a gas-tight, two-chamber H-cell. The working compartment contained the working electrode and reference electrode submerged in a CO$_2$-saturated solution containing 0.3 mM of [Co(PDI-Py)], 0.1 M nBu$_4$NPF$_6$, and 11 M H$_2$O in MeCN. For experiments with added amines, the concentration of the amine was 0.05 M. The auxiliary compartment contained the auxiliary electrode submerged in the same solution but with 5 mM Fc added as a sacrificial reductant.

experiments showed little precipitation of cobalt onto the electrode surface, suggesting there is minimal catalyst decomposition during the CPE experiments (Table 2, Fig. S26–S31, ESI†). Note that CPEs conducted at the more negative potential of -2.34 V $vs.$ Fc$^{+/0}$ in identically prepared CO$_2$-saturated solutions with 11 M H$_2$O, 0.05 M NBA, and 0.03 M [Co(PDI-Py)] show primarily H$_2$ production with FE$_{H2} \sim 84\%$ and FE$_{CO} \sim 12\%$ (Fig. S32 and Table S3, ESI†), consistent with our previous studies.[17]

To understand the CO$_2$-reactive species and its interaction with the Co-catalyst, we performed a series of spectroscopic studies. To determine whether this coordination persists for more reduced complexes, we studied the interaction of carbamates with the [Co(PDI-Py)]$^{2+}$ complex by UV-Vis experiments. In our electrocatalytic experiments, the Co(III) complex [Co(PDI-Py)]$^{3+}$ is first reduced to the Co(II) complex [Co(PDI-Py)]$^{2+}$ $in\ situ$ to enter the catalytic cycle.[17] The UV-Vis spectra of independently prepared [Co(PDI-Py)Br$_2$] complex in N$_2$-sparged electrolyte solution (Fig. 3, blue line) shows three absorption features at 550 nm, 465 nm, 365 nm. Upon saturating this solution with CO$_2$, there is no change in the absorption peaks from the N$_2$-sparged solution, confirming that CO$_2$ does not coordinates with [Co(PDI-Py)Br$_2$] (Fig. 3, purple line). We next collected a UV-Vis spectrum of the [Co(PDI-Py)Br$_2$] complex in a N$_2$-sparged solution containing NBA (Fig. 3, red line). We observe a blue shift in the absorption spectrum compared to the parent system without NBA present, and we interpret this shift as a result of coordination of NBA to the [Co(PDI-Py)]$^{2+}$ complex. Sparging the NBA-containing solution with CO$_2$ results in a noticeable change in the UV-Vis spectrum, with a disappearance of the absorption peak at ~ 480 nm and the emergence of a new absorption peak at ~ 350 nm (Fig. 3, green line). We interpret this change in the spectrum to indicate that CO$_2$ is reacting with NBA in solution forming n-butylcarbamate (NBA-CO$_2$), and this NBA-CO$_2$ is then coordinating to the [Co(PDI-Py)]$^{2+}$ active catalyst (Fig. S33, ESI†). The formation of NBA-CO$_2$ in CO$_2$-sparged MeCN containing NBA was confirmed through NMR and FTIR studies (Fig. S34 and S35, ESI†). The key result from these studies is that the carbamate formed

Fig. 3 Absorption measurements of 0.1 mM [Co(PDI-Py)Br$_2$] in MeCN solutions containing 0.03 M nBu$_4$NPF$_6$ and 11 M H$_2$O in N$_2$-sparged solution (blue line), CO$_2$-saturated solution (purple line), N$_2$-sparged solution with 6.6 mM NBA (red line), and CO$_2$-saturated solution with 6.6 mM NBA (green line).

in situ coordinates to the [Co(PDI-Py)]$^{2+}$ complex, something that was not observable from the CVs.

Motivated by our spectroscopy results, we conducted CPE experiments of [Co(PDI)Py] in Ar-sparged MeCN electrolyte solution with 11 M H$_2$O containing the commercially-available carbamate salt dimethylammonium dimethylcarbamate (DMA-CO$_2$) as our sole CO$_2$ source. Under these conditions, we observed lower selectivity and activity for CO formation: FE$_{CO}$ ≈ 16% with only 1.9 C of charge passed (Table S4, ESI†). This lower activity for the carbamate compared to the CO$_2$-saturated amine solution could be a consequence of the equilibria processes in Scheme 1b: without additional CO$_2$ present in the system, the added carbamate may dissociate to form free DMA and the corresponding bicarbonate compound.

Because of inferior activity for CO production using DMA-CO$_2$ as the sole CO$_2$ source, we wanted to determine whether the *in situ* formation of a carbamate is important for the observed catalytic activity. We studied the electrocatalytic activity for CO production by [Co(PDI-Py)] in CO$_2$ saturated solutions with 11 M H$_2$O using aniline as the amine source. Aniline does not form stable carbamate species upon reaction with CO$_2$ due to aniline's comparatively low nucleophilicity.[18] CVs of [Co(PDI-Py)] in the presence of 0.02 M aniline and CO$_2$ saturated electrolyte solution show no shift in redox potentials for the Co$^{3+/2+}$ and Co$^{2+/+}$ compared to CVs of [Co(PDI-Py)] in aniline-free solvent (Fig. S10, ESI† and Table 1). Similarly, E_{onset} is the same in the absence or presence of aniline, and no increase in catalytic activity was observed ($i_{c,amine}/i_c$ = 1). Overall, these results suggest that *in situ* carbamate production by amine-CO$_2$ reaction plays an important role in enhancing catalytic activity for the e-CO$_2$RR by [Co(PDI-Py)] catalyst. The carbamate species is likely acting as an active substrate for CO$_2$RR to CO.[12,19,20] However, we cannot entirely rule out the possibility that CO$_2$ is the active species for reduction to CO, and that the *in situ* formed carbamate is acting as a delivery mechanism for CO$_2$ to the catalyst.[21]

In conclusion, we have shown that adding amines to CO$_2$-saturated MeCN solutions containing the catalyst [Co(PDI-Py)] and

11 M H$_2$O as a proton source leads to an increase in the e-CO$_2$RR activity for CO production. CO$_2$ reacts with the amines in solution, generating *in situ* alkyl-carbamate species. UV-Vis and electrochemical studies suggest that this carbamate species interacts with the [Co(PDI-Py)] complex, and is likely the active substrate for CO production. Aniline which cannot form carbamate salts, doesn't enhance the catalytic activity. Overall, these findings can be a useful starting point for the development of efficient electrocatalytic systems for electrochemical reactive capture of CO$_2$.

Data availability

The data supporting this article have been included as part of the ESI.†

Conflicts of interest

There are no conflicts to declare.

Notes and references

1 M. Bui, C. S. Adjiman, A. Bardow, E. J. Anthony, A. Boston, S. Brown, P. S. Fennell, S. Fuss, A. Galindo, L. A. Hackett, J. P. Hallett, H. J. Herzog, G. Jackson, J. Kemper, S. Krevor, G. C. Maitland, M. Matuszewski, I. S. Metcalfe, C. Petit, G. Puxty, J. Reimer, D. M. Reiner, E. S. Rubin, S. A. Scott, N. Shah, B. Smit, J. P. M. Trusler, P. Webley, J. Wilcox and N. Mac Dowell, *Energy Environ. Sci.*, 2018, **11**, 1062–1176.
2 E. Sanchez Fernandez, E. L. V. Goetheer, G. Manzolini, E. Macchi, S. Rezvani and T. J. H. Vlugt, *Fuel*, 2014, **129**, 318–329.
3 R. E. Siegel, S. Pattanayak and L. A. Berben, *ACS Catal.*, 2023, **13**, 766–784.
4 A. M. Appel and J. Y. Yang, *ACS Energy Lett.*, 2024, **9**, 768–770.
5 S. Kar, A. Goeppert and G. K. S. Prakash, *Acc. Chem. Res.*, 2019, **52**, 2892–2903.
6 S. Sun, H. Sun, P. T. Williams and C. Wu, *Sustainable Energy Fuels*, 2021, **5**, 4546–4559.
7 S. Wang and X. Wang, *Angew. Chem., Int. Ed.*, 2016, **55**, 2308–2320.
8 E. Fujita, D. C. Grills, G. F. Manbeck and D. E. Polyansky, *Acc. Chem. Res.*, 2022, **55**, 616–628.
9 I. Sullivan, A. Goryachev, I. A. Digdaya, X. Li, H. A. Atwater, D. A. Vermaas and C. Xiang, *Nat. Catal.*, 2021, **4**, 952–958.
10 S. E. Jerng and B. M. Gallant, *iScience*, 2022, **25**, 104558.
11 J. Bi, P. Hou, F.-W. Liu and P. Kang, *ChemSusChem*, 2019, **12**, 2195–2201.
12 H. Kumagai, T. Nishikawa, H. Koizumi, T. Yatsu, G. Sahara, Y. Yamazaki, Y. Tamaki and O. Ishitani, *Chem. Sci.*, 2019, **10**, 1597–1606.
13 D. C. Grills, Y. Matsubara, Y. Kuwahara, S. R. Golisz, D. A. Kurtz and B. A. Mello, *J. Phys. Chem. Lett.*, 2014, **5**, 2033–2038.
14 M. Bhattacharya, S. Sebghati, R. T. VanderLinden and C. T. Saouma, *J. Am. Chem. Soc.*, 2020, **142**, 17589–17597.
15 C. G. Margarit, N. G. Asimow, C. Costentin and D. G. Nocera, *ACS Energy Lett.*, 2020, **5**, 72–78.
16 J. B. Jakobsen, M. H. Rønne, K. Daasbjerg and T. Skrydstrup, *Angew. Chem., Int. Ed.*, 2021, **60**, 9174–9179.
17 W. Nie, D. E. Tarnopol and C. C. L. McCrory, *J. Am. Chem. Soc.*, 2021, **143**, 3764–3778.
18 P. V. Kortunov, M. Siskin, L. S. Baugh and D. C. Calabro, *Energy Fuels*, 2015, **29**, 5919–5939.
19 A. Khurram, L. Yan, Y. Yin, L. Zhao and B. M. Gallant, *J. Phys. Chem. C*, 2019, **123**, 18222–18231.
20 G. Lee, Y. C. Li, J.-Y. Kim, T. Peng, D.-H. Nam, A. Sedighian Rasouli, F. Li, M. Luo, A. H. Ip, Y.-C. Joo and E. H. Sargent, *Nat. Energy*, 2021, **6**, 46–53.
21 G. Leverick, E. M. Bernhardt, A. I. Ismail, J. H. Law, A. Arifutzzaman, M. K. Aroua and B. M. Gallant, *ACS Catal.*, 2023, **13**, 12322–12337.